Available online at www.sciencedirect.com

ScienceDirect

Procedia Engineering 109 (2015) 285 – 295

Procedia Engineering

www.elsevier.com/locate/procedia

XXIII Italian Group of Fracture Meeting, IGFXXIII

Numerical evaluation and experimental comparison of elasto-plastic stress-strain distribution around the corner cracks of a notched specimen

Raffaele Sepe[a]*, Enrico Armentani[a], Francesco Caputo[b], Giuseppe Lamanna[b]

[a]*Department. of Chemical, Materials and Production Engineering - University of Naples Federico II - P.le V. Tecchio, 80 - 80125 Naples, Italy*
[b]*Department of Industrial and Information Engineering - Second University of Naples - Via Roma 29 - 81031 Aversa, Italy*

Abstract

This paper concerns the numerical simulations, by a commercial FEM code, related to notched specimens experimentally tested by neutron diffraction and synchrotron radiation diffraction, in order to correlate the deformation states around the crack tip. Two cracked specimens were analyzed. In one case a long crack has been induced into the specimen, which has been investigated subsequently by neutron diffraction technique. In the other case a smaller crack was induced, which has been investigated by synchrotron radiation diffraction technique. The numerical and experimental results are substantially in good agreement. However some differences can be observed; the reason can be found in the microscopic structure and particular history of the material under load.

Peer-review under responsibility of the Gruppo Italiano Frattura (IGF)

Keywords: cracks; FEM; non-linear analysis, neutron diffraction technique, synchrotron radiation diffraction technique;

1. Introduction

For life time prediction of flawed structures, the effect of geometry of the components and its interaction with growing cracks should be considered. Generally numerical methods such as Finite Element Method (FEM) [1-3] and Boundary Element Method (BEM) [4-7] can be used for evaluation of crack growth parameters when modeling a

* Corresponding author. Tel.: +39-081-768-24-50; fax: +39-081-768-21-72
E-mail address: raffsepe@unina.it

Peer-review under responsibility of the Gruppo Italiano Frattura (IGF)
doi:10.1016/j.proeng.2015.06.235

complex shape and the continuously changing path of the growing crack. It is generally recognized that residual strength evaluation in thin metal sheets such as aircraft panels requires consideration of yielding behaviour.

The analysis methods generally used in residual strength calculations are limited mostly to linear elastic fracture mechanics (LEFM) [8] due to the lack of tested and validated non-linear analysis methods for aircraft panels. LEFM models can lead to conservative designs, which in turn can lead to an increase in aircraft weight and can result in more inspections to be scheduled than necessary and more costly tests. In order to reduce costs and gain a better understanding of crack behaviour, it is important to develop more efficient analysis techniques specifically well suited for aircraft panels. These methods should be capable of dealing with yielding due to cracking as well as rivet and stiffener failures. In the last years, several researchers have considered the plastic zone size at the crack tip [9-16].

This paper concerns the numerical simulations, by a commercial FEM code, related to notched specimens experimentally tested by neutron diffraction and synchrotron radiation diffraction, in order to correlate the deformation states around the crack tip. Two cracked specimens were analyzed. In one case a long through crack was induced in the specimen, which has been subsequently investigated by using neutron diffraction technique. In the other case a smaller crack was induced, which has been investigated by synchrotron radiation diffraction technique.

This activity has been carried out through some steps which can be summarized as follows: generating cracks by fatigue notched specimens made in aluminium alloy 2024-T3; detecting their crack sizes and shapes; FEM analysis in linear elastic material condition to calculate SIF's and so to define the refinement of the mesh; FEM analysis in non linear material condition to investigate the effect of yielding at crack tip.

The numerical and experimental results are substantially in good agreement. However some differences can be observed; the reason can be found in the microscopic structure and particular history of the material under load. In fact the material grains show a highly preferred orientation in the neighborhood of the notch, due to the mechanical cut procedures, moreover the microscopic structure can be different from other zones of the material, and also point-dependent.

2. Experimental test

The specimens employed in this study were rectangular single edge notched specimens (4 mm thickness) as shown in Fig. 1 The material used for the experimental work was aluminium alloy 2024-T3 whose mechanical properties are given in Table 1. The material was delivered as flats in the dimensions 2000x100x4 mm^3 and the specimens were extracted in the longitudinal direction. After grinding, the notch area has been mechanically and electrochemically polished. The finishing operation was done with the aid of a polishing felt and diamond paste with a grain size in the range of 0.5÷1 mm.

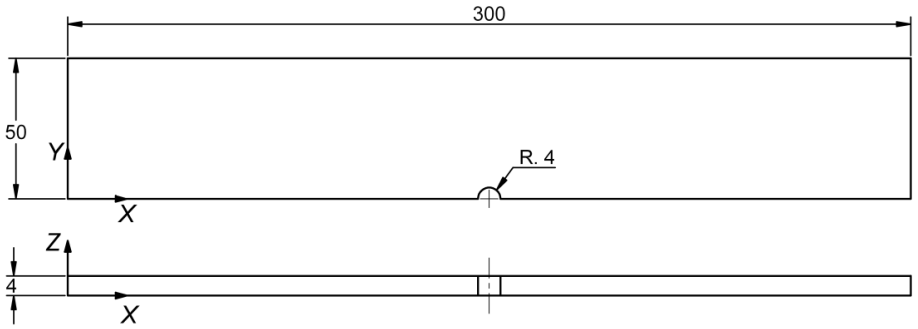

Fig. 1. Specimen geometry.

The fatigue tests have been carried out on closed loop servohydraulic testing systems. The specimens are clamped using hydraulic grips and axially loaded in constant amplitude load control (R = 0.05, P_{max} = 16.5 kN).

After reaching a surface crack length of about 2 mm in the notch root, the experiment was terminated (Fig. 2). Two type cracked specimens were obtained. In one case a long through crack has been induced, which has been investigated subsequently by neutron diffraction technique [17]. In the other case a short crack was induced, which was investigated by synchrotron radiation diffraction technique [17]. Actually, after cracking, the specimen with long through crack has been subjected to static load (P = 9 kN) and then the strain field was measured by neutron diffraction technique, while the specimen with short crack has been subjected to static load (P = 18 kN) and then the strain field has been measured by synchrotron radiation diffraction technique.

Table 1. Mechanical properties of 2024-T3.

Property	Value
Young's modulus	73000 [MPa]
Tensile Strength	483 [MPa]
Yield Strength	345 [MPa]
Poisson ratio	0.33

The crack shapes and sizes have been taken by a digital camera mounted on a light-optical microscope. Crack measurements were done by using an image processing software. In order to determine the crack depth an associated to the surface crack length, the specimens had been deep-frozen in liquid nitrogen and broken open.

Micrographs taken by a scanning electron microscope showed that in the specimen with a long crack the front was highly irregular (Fig. 2.a), while in the specimen with a short crack the fatigue fracture surface was almost semicircular (Fig. 2.b). The numerically simulations are then based on the assumption that the long through crack has the front of crack shown in Fig. 3.a while the short crack has a semicircular crack shape also shown in Fig. 3.b.

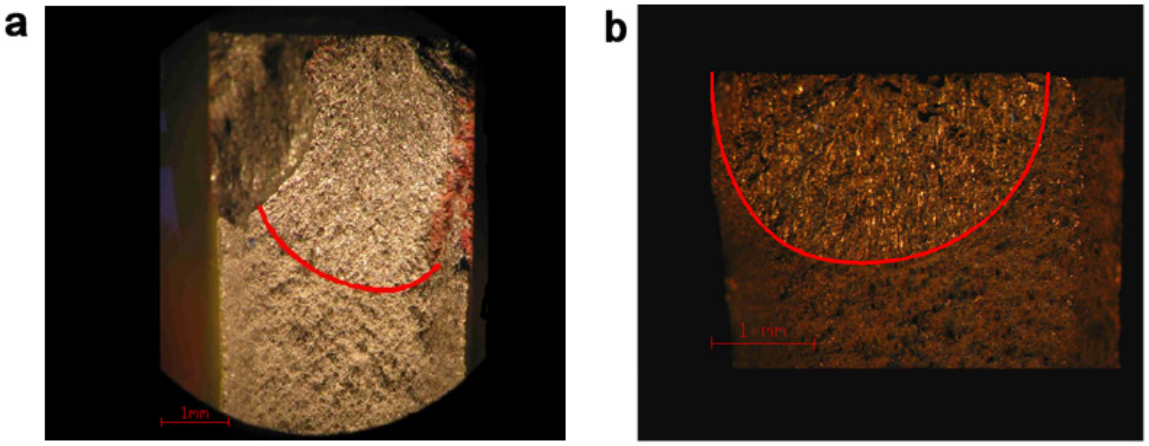

Fig. 2. (a) front of the long through crack; (b) front of the short crack.

3. Numerical model of the specimen with long through crack

A linear analysis has been carried out with different models in order to individuate an h-convergent mesh; furthermore, a non linear simulation has been carried out to evaluate the stress-strain state around the crack tip. In the linear analysis a study on stress intensity factors (SIF's) along the crack front has been carried out too.

The simulations are performed by ANSYS code, which is able to perform both linear and non linear analyses and has an internal post-process routine for the determination of SIF's.

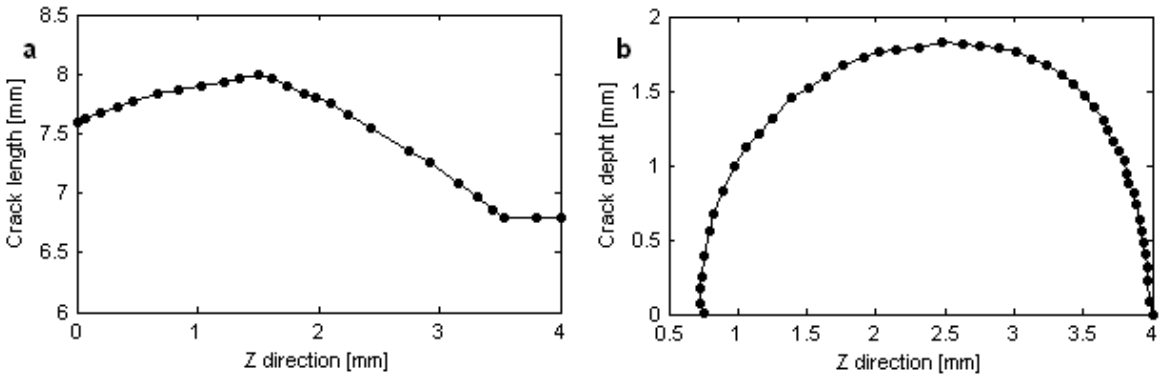

Fig. 3. (a) dimensions of long through crack; (b) dimensions of short crack.

3.1. Linear analysis

The initial numerical analyses were aimed to the assessment of a convergent FEM model. An iso-parametric 20 nodes element (Solid 95) with three degree of freedom for each node, well suited for calculating the SIF's, is used for the analysis.

The model has been constrained at one end in X and Y direction, at the other end a load of P = 20 kN has been applied in X direction. Z direction constraints have been applied too, in order to prevent rigid body displacements. The crack front has been modeled with quarter point elements in wedge configuration to simulate stress singularity at crack tip and evaluate the SIF's. Wedge elements are present only at crack tip; all the others elements in the model have hexahedral shape; so, it was possible to divide the whole solid in a great number of hexahedral volumes with regular form. In Figs. 4.a and 4.b are shown respectively a detail of crack modeling and a detail of mesh on the crack plane.

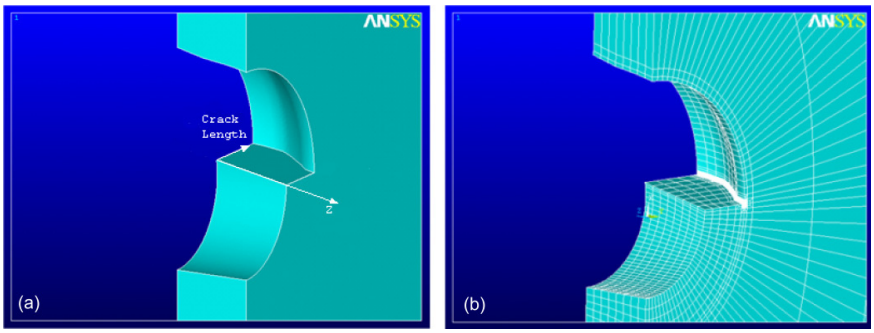

Fig. 4. (a) detail of crack modeling; (b) detail of mesh on the crack plane.

To contain computational effort a sub-modeling technique has been applied; with this approach it has been possible to model for example 64 elements on the crack front so reducing the computational time of about 60% with respect to a chosen 32 elements model (without sub-modeling).

In order to run the sub-model correctly, nodal results of the full-scale model with 32 elements have been used selecting and re-meshing only the reduced volume near the notch. For the convergence study of the whole mesh four models were built, including the sub-model, three related to the full domain, while the fourth related to the sub-model; the details are presented in Table 2.

Table 2. Details of FEM models.

	Model 1	Model 2	Model 3	Model 4
Elements on front crack	8	16	32	64
Nodes	58479	129727	257561	-
Elements	12624	29584	60128	-

For each simulation the computation of the SIF's has been carried out, because this parameter has been used to individuate the convergence mesh. In Fig. 5 are shown the SIF's values for each model. As the model with 32 elements (model 3) and 64 elements (model 4) give the same results in the next we will use the model 3.

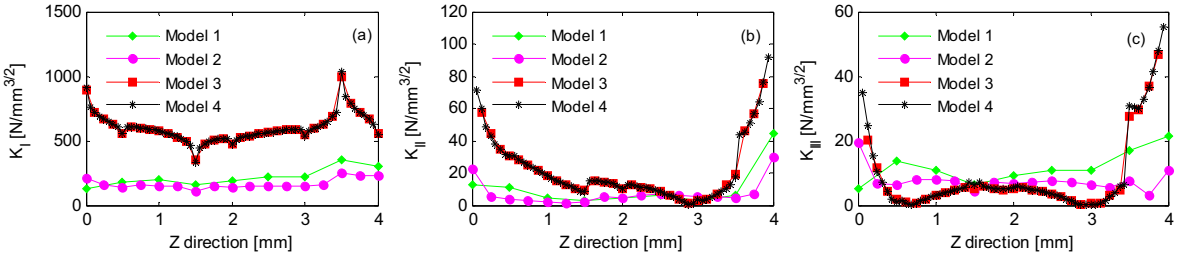

Fig. 5. (a) K_I SIF's along crack front; (b) K_{II} SIF's along crack front; (c) K_{III} SIF's along crack front.

3.2. Non linear analysis

Once detected the convergent model, a non linear material analysis has been carried out in order to investigate the effect of yielding at the crack tip. In order to correlate numerical results with neutron diffraction tests, some simulations have been carried out with the same boundary conditions of the experimental tests. The model has been constrained at one end in X and Y direction while on the other a load of $P = 9$ kN has been applied in X direction; Z direction constraints have been applied too, in order to prevent rigid body displacement. The material has been modeled as bilinear with kinematic hardening, being mechanical properties are reported in Table 1.

4. Numerical model of the specimen with short crack

Also here, the element used for the analysis is an iso-parametric element with 20 nodes (Solid 95). The used material is the same as the first case. In order to correlate numerical results with synchrotron radiation diffraction tests, some non linear analyses have been carried out with the same boundary conditions of the experimental tests. The model has been constrained at one end in X and Y direction while on the other an axial load of $P = 18$ kN has been applied in X direction; Z direction constraints have been applied too, in order to prevent rigid body displacement.

4.1. Convergence analysis

Several models with different numbers of elements on the crack front were generated. All the elements in the model have a hexahedral shape. The successive refinement of the mesh has concerned specifically the same containing the cracked notched part.

However, in order to increase the refinement of the mesh without increase the computational time, a sub-modeling technique has been applied too; with this approach it has been possible to put more elements on the crack front. To perform the sub-model, nodal displacement results of the last full-scale model have been used far from the cut sections. So in whole for mesh convergence study six models were built, including the sub-models; the details

are reported in Table 3 and 4. As shown in the tables, the parameters used to individuate the convergent mesh are von Mises equivalent stress and maximum normal stress in Z direction.

Table 3. Details of FEM full models.

	Model 1	Model 2	Model 3
Nodes	95309	245983	284811
Elements	21896	57976	67452
Nodes on the crack front	65	97	97
Elements on the crack front	32	48	48
Elements along notch	28	36	42
von Mises $\sigma_{eq\ max}$ [MPa]	361	369	396
$\sigma_{z\ max}$ [MPa]	515	562	685

Table 4. Details of FEM sub-models.

	Sub-model 4	Sub-model 5	Sub-model 6
Nodes	185301	409179	471407
Elements	43776	97812	112944
Nodes on the crack front	97	129	129
Elements on the crack front	48	129	129
Elements along notch	32	38	52
von Mises $\sigma_{eq\ max}$ [MPa]	400	416	421
$\sigma_{z\ max}$ [MPa]	738	790	800

5. Results and discussion

5.1. Specimen with long through crack

In Fig. 6 the von Mises stress fields around the corner crack are shown. Due to the low level of the applied load, the yielding effect is very limited.

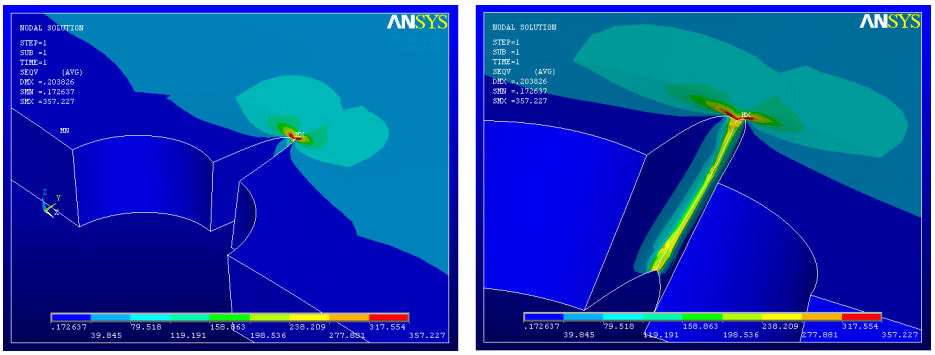

Fig. 6. Detail of sub-model with 64 elements on crack front and 38 elements along the notch.

Furthermore longitudinal and transversal strains depending on the external loading direction have been evaluated in some points along a line parallel to the crack propagation and on the mean plane of the plate (Z = 2 mm), as shown in Fig. 7. For each point two values have been evaluated: a local value that is the nodal strain value of the node nearest the measure point and the strain mean value related to nodes contained in a volume centered at the measure point and with sizes 0.8x0.5x1 mm^3, that is the experimental measure volume (Fig. 8).

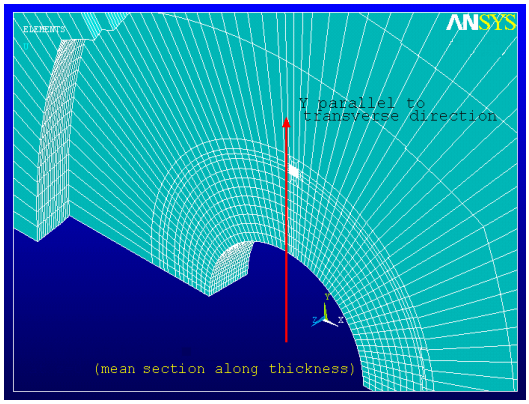

Fig. 7. Direction of the measurements (plane Z = 2 mm).

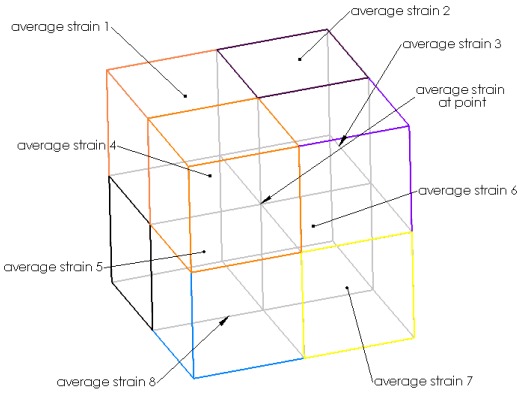

Fig. 8. Volumes to evaluate the average value of the strain.

Then the average strain has been calculated by a routine that divided the volume in eight parts and estimated the average strain as arithmetic mean of the strains evaluated in each part,

$$\varepsilon_{av} = \frac{\sum_{i=1}^{8} \varepsilon_{av_i}}{8} \tag{1}$$

where ε_{av} is the mean strain value of the volume and ε_{avi} is the strain value of each part of the volume.

This approach has been necessary because the nodes were not uniformly distributed in the volume so that a simple arithmetic mean would not be a representative value. It was not possible to evaluate local values for locations distant more than 8.5 mm from the crack, because there were not nodes close to those points, so that only average values were evaluated. In order to determine the stresses, by assuming a biaxial state, longitudinal and transversal stresses can be computed by Hooke laws.

In the Figs. 9 and 10 the numerical results have been compared with results of neutron diffraction tests in terms of strains and stresses respectively.

It can be observed that the differences between local and average strains increase near the crack tip; this is because in this zone there are high strain gradients so that in the measure volume the distribution of the strain is not uniform. Moreover the trend of numerical results appears more regular and present a pick near to the crack tip. Instead, the experimental results, appear less regular and present high negative values in the zone far from the crack tip.

The results of neutron diffraction measurements (long crack) are in general in good agreement with FEM simulation. Nevertheless, the experimental data show the following features:

- a compression state is measured in the neighborhood of the crack tip, especially in the transverse direction (about parallel to the crack direction);
- the strain/stress values show oscillations as a function of the distance from the crack tip.

These effects generally are due:

- the neutron measurements are carried out averaging on a relatively wide gauge volume (0.8x0.5x1 mm^3);
- it is also to be noticed that previous measurements carried out by other authors [18-19] have detected compressive stresses in the neighborhood of the crack tip in cracked steel specimens under external loading. This could be explained with the presence of residual stresses pre-existing before the crack was initiated, due for instance to the cut of the notch;
- as shown in Fig. 11, microscopic structure of the material shows a highly preferred orientation for the material grains, in the neighborhood of the notch, due to the mechanical cut procedures. Moreover this microscopic structure can be different from that of other zones of the material, and also point-dependent.

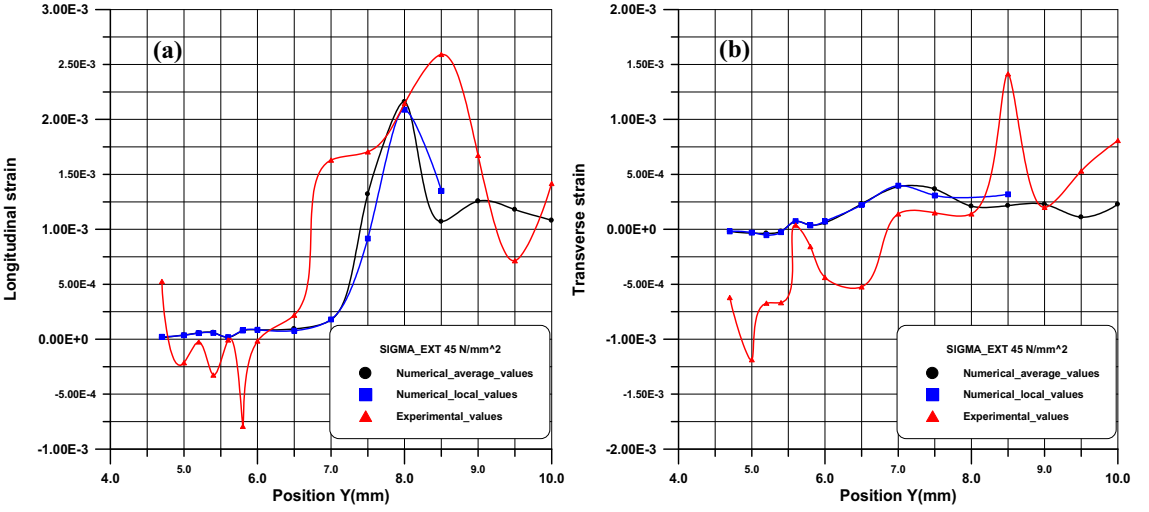

Fig. 9. (a) longitudinal strains ; (b) transverse strains.

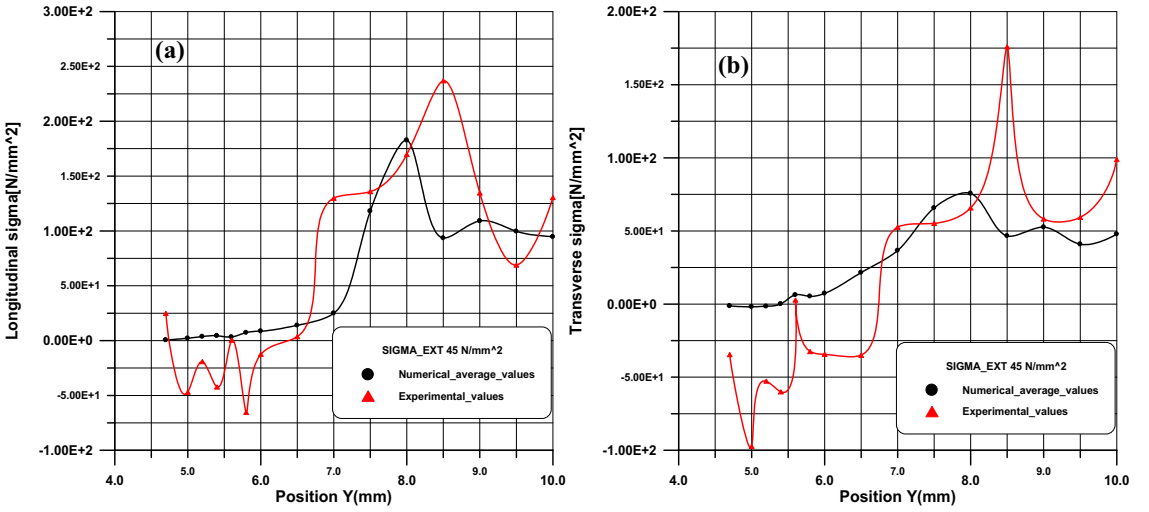

Fig. 10. (a) longitudinal stresses ; (b) transverse stresses.

5.2. Specimen with short crack

In this case the numerical results of FEM analysis have been compared with the results of synchrotron radiation diffraction technique; it has been necessary to localize specific measure points. In Fig. 12 are shown the points where the longitudinal and transversal strains were measured with synchrotron radiation diffraction technique. The measurements were carried out in the three different planes at Z = 0 mm, Z = 2 mm and Z = 4 mm.

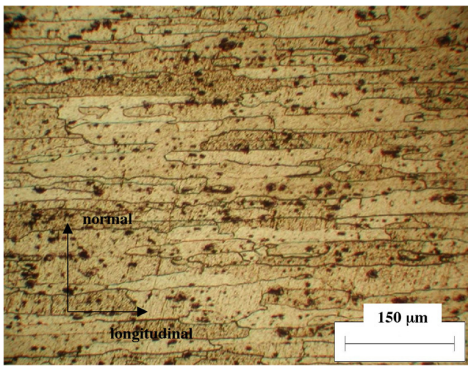

Fig. 11. Microstructure of the material around the crack.

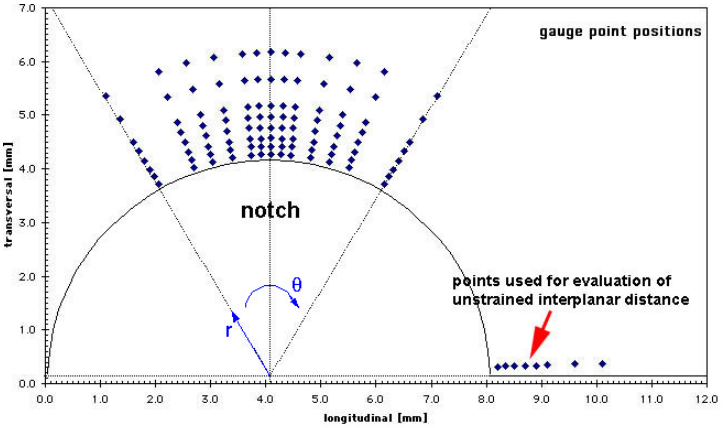

Fig. 12. Points around the notch where the strains have been measured with synchrotron radiation diffraction technique.

The Fig. 13 shows the correlation between numerical and experimental results.

For each point two numerical values were determined: a local value (red line) that is the strain value of the node nearest the measure point and an average value (blue line) that is the mean value of the strain values of nodes contained in a volume centered at measure point, with size of 0.1x0.1x1.5 mm^3.

Some differences between numerical and experimental results can be observed; the reason can be found, as stated for the first case, in the microscopic structure and in the particular history of the material under load. The presence of a highly preferred orientation of the material grains greatly influences the results of the synchrotron radiation measurements. In fact as shown in Fig. 14, the microstructure of the material influences the measurements. In the unloaded case relative intensities of the peaks should be different, e.g. (111) peak should be more intense than (200). Moreover the microstructure is changed by the external loading e.g. (311) peak disappears in the loaded case.

6. Conclusion

The numerical and experimental results are substantially in good agreement. However, some differences can be observed; the reasons can be found both in the microscopic structure and in the particular history of the material under load.

The neutron measurement results, even though influenced by microstructure, are referred to an “experimental average” over a wide material volume (i.e. many grains).

The synchrotron radiation results are referred to a much narrower beam spot (0.1x0.1 mm^2). Therefore the average is made over a lower number of grains and then it is more influenced by the particular microstructure of the zone where the beam is probing the material.

The compressive strain states experimentally detected could be attributed to already existing residual stress in the neighborhood of the notch, probably due to the cutting procedure used to obtain it.

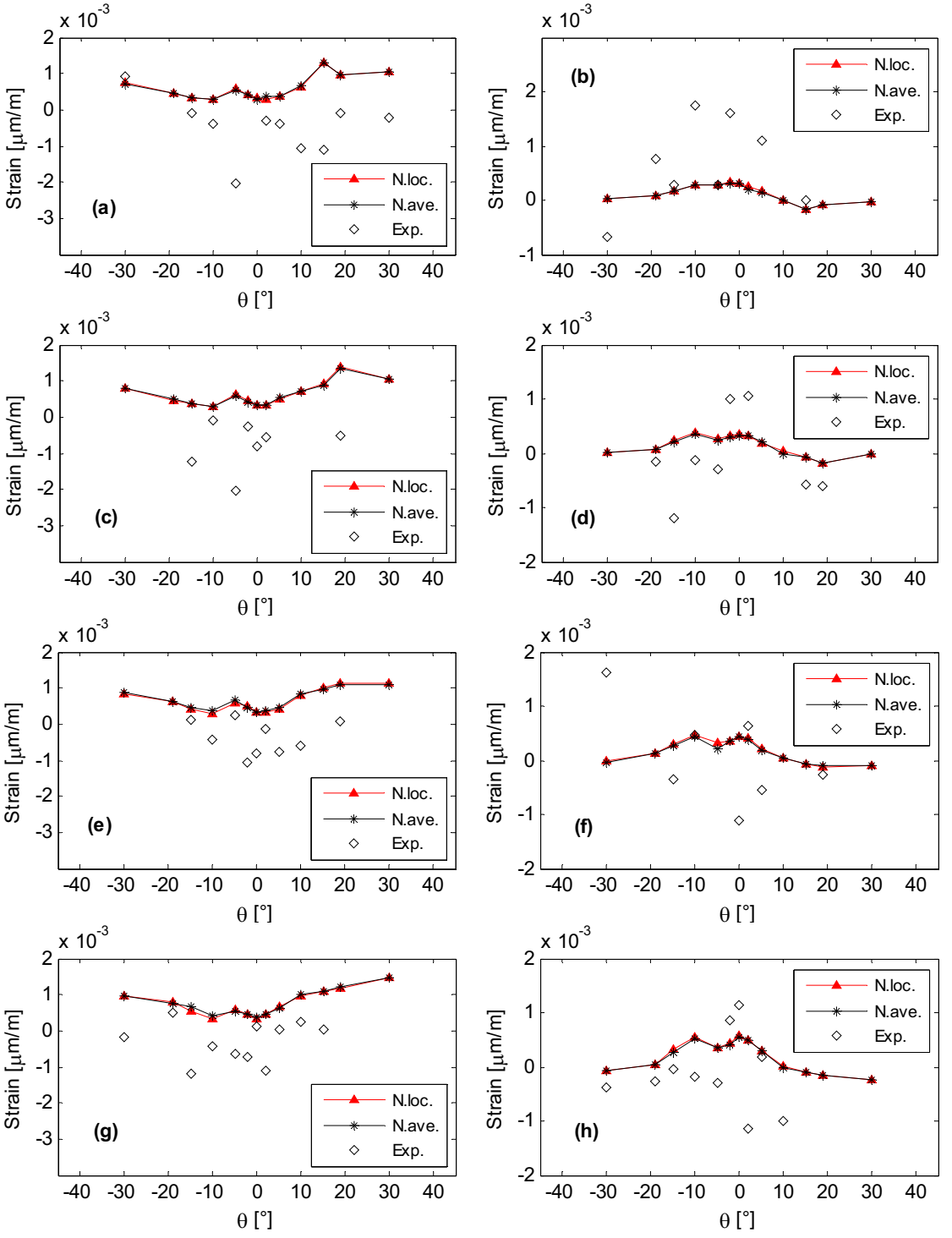

Fig. 13. (a) longitudinal strain at r = 4.4 mm and Z = 2 mm; (b) transverse strain at r = 4.4 mm and Z = 2 mm; (c) longitudinal strain at r = 4.6 mm and Z = 2 mm; (d) transverse strain at r = 4.6 mm and Z = 2 mm; (e) longitudinal strain at r = 4.8 mm and Z = 2 mm; (f) transverse strain at r = 4.8 mm and Z = 2 mm; (g) longitudinal strain at r = 5.0 mm and Z = 2 mm; (h) transverse strain at r = 5.0 mm and Z = 2 mm.

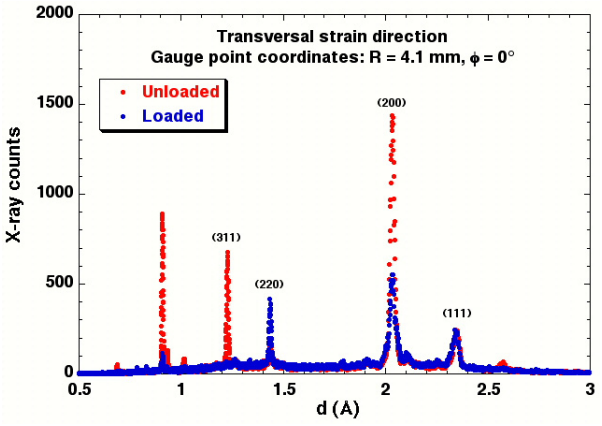

Fig. 14. Diffraction patterns obtained in the synchrotron radiation experiment.

References

[1] K. Nasri, M. Abbadi, M. Zenasni, M. Ghammouri, Z. Azari, Double crack growth analysis in the presence of a bi-material interface using XFEM and FEM modelling, Engineering Fracture Mechanics, 132 (2014) 189-199.
[2] A. Materna, V. Oliva, Elastic-plastic FEM investigation of the thickness effect on fatigue crack growth, Procedia Eng., 10 (2011) 1109-1114.
[3] J.B. Esnault, V. Doquet, P. Massin, A three-dimensional analysis of fatigue crack paths in thin metallic sheets, Int. J. of Fatigue, 62 (2014) 119-132.
[4] R. Citarella, G. Cricrì, E. Armentani, Multiple crack propagation with Dual Boundary Element Method in stiffened and reinforced full scale aeronautic panels, Key Engineering Materials 560 (2013) 129-155.
[5] R. Citarella, M. Lepore, J. Fellinger, V. Bykov, F. Schauer, Coupled FEM-DBEM method to assess crack growth in magnet system of Wendelstein 7-X, Fracture and Structural Integrity (Frattura ed Integrità Strutturale) 26 (2013) 92-103.
[6] R. Citarella, G. Cricrì, M. Lepore, M. Perrella, Thermo-Mechanical Crack Propagation in Aircraft Engine Vane by Coupled FEM-DBEM Approach, Advances in Engineering Software 67 (2014) 57-69.
[7] R. Citarella, M. Lepore, V. Shlyannikov, R. Yarullin, Fatigue surface crack growth in cylindrical specimen under combined loading, Engineering Fracture Mechanics 131 (2014) 439–453.
[8] C. Calì, R. Citarella, Residual strength assessment for a butt joint in MSD condition, Advances in Engineering Software 35 (2004) 373-382.
[9] Yu.G. Matvienko, The Effect of the Non-singular T-stress Components on Crack Tip Plastic Zone under Mode I Loading, Procedia Materials Science, 3 (2014) 141-146.
[10] F. Caputo, A. De Luca, G. Lamanna, A. Soprano, Numerical study of a plate with a pre-cracked circular notch, Key Engineering Materials 627 (2015) 101-104.
[11] Huang Yi, Chen Jingjie, Liu Gang, A new method of plastic zone size determined based on maximum crack opening displacement, Eng. Fracture Mechanics 77 Issue 14 (2010) 2912-2918.
[12] F. Caputo, G. Lamanna, L. Lanzillo, A. Soprano, Numerical investigation on LEFM limits under LSY conditions, Key Engineering Materials 577-578 (2014) 381-384.
[13] F. Caputo, G. Lamanna, A. Soprano, On the evaluation of the plastic zone size at the crack tip, Eng. Fracture Mechanics 103 (2013) 162-173.
[14] S.C. Mishra, B.K. Parida, Determination of the size of crack-tip plastic zone in a thin sheet under uniaxial loading, Eng. Fracture Mechanics 22 Issue 3, (1985) 351-357.
[15] F. Caputo, G. Lamanna, A. Soprano, An Analytical Formulation for the Plastic Deformation at the Tip of Short Cracks, Procedia Engineering 10 (2011) 2988-2993.
[16] R. Sethuraman, S. Viswanadha Gupta, Evaluation of notch root elasto-plastic stress–strain state for general loadings using an elastic solution, Int. J. of Pressure Vessels and Piping 81 Issue 4 (2004) 313-325.
[17] G. Anatriello, E. Armentani, F. Caputo, R. Esposito, G. Godono, A. Soprano, Advanced Design Concepts and Maintenance by Integrated Risk Evaluation for Aerostructures, WP5.2: Round robin tests, ADMIRE-TR-5.2-97-3.1/UNAP (2004).
[18] M. Ceretti, C.A. Hippsley, M.T. Hutchings, A. Lodini, Colin Windsor, Neutron diffraction measurement of the triaxial stress field in a fatigued test specimen, Physica B 234 (1997) 969-971.
[19] K. Hirschi, M. Ceretti, B. Marini, J.M. Sprauel, Residual stresses and hardening near crack tip regions of austenitic fatigue specimens, Applied Physics A, 74 (2002) 1722-1724.